Heliyon 10 (2024) e34665

Contents lists available at ScienceDirect

Heliyon

journal homepage: www.cell.com/heliyon

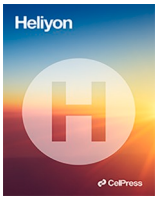

Research article

Preparation and stability investigation of ultrasound-assisted W/O/W multiple nanoemulsions co-loaded with hydrophobic curcumin and hydrophilic arbutin for tyrosinase inhibition

Mathukorn Sainakham [a,b,*], Bouachompoo Promma [a], Arthima Ngernthong [a], Kanokwan Kiattisin [a], Korawinwich Boonpisuttinant [c], Krisada Wuttikul [d], Pensak Jantrawut [a,b], Warintorn Ruksiriwanich [a,b]

[a] *Department of Pharmaceutical Sciences, Faculty of Pharmacy, Chiang Mai University, Chiang Mai, 50200, Thailand*
[b] *Cluster of Valorization and Bio-Green Transformation for Translational Research Innovation of Raw Materials and Products, Chiang Mai University, Chiang Mai, 50200, Thailand*
[c] *Innovative Natural Products from Thai Wisdoms (INPTW), Faculty of Integrative Medicine, Rajamangala University of Technology, Thanyaburi, Pathumthani, 12130, Thailand*
[d] *Division of Cosmetic Science, School of Pharmaceutical Sciences, University of Phayao, Phayao, 56000, Thailand*

ARTICLE INFO

Keywords:
Nanoemulsion
Tyrosinase inhibition
Anti-melanogenesis
Cytotoxicity
Stability test

ABSTRACT

In the present, whitening products are most popular in the cosmetics market, and nanoemulsions are effective drug delivery systems through the skin. The objective of this study was to investigate multiple nanoemulsion formulations for lightning skin effects. The method of this study was the selection of active compounds based on synergistic tyrosinase inhibition activity, formulation preparation by low and high energy methods, physicochemical property determination, stability test, cell toxicity, and anti-melanogenesis in cell culture. From the results, it was found that tyrosinase inhibition with substrate l-tyrosine from the mixture of curcumin and alpha-arbutin gave the highest activity with an IC_{50} of 63.58 ± 4.99 μM, showed a synergistic effect at a CI value of 0.99, and selected these compounds to develop formulations by the low energy method. However, the most formulations prepared by this method were unstable and phase separated, while the high energy method gave the most formulations with good properties, which were selected for further investigation. The best formulation was 2DS which showed internal droplet morphology in the range of nanometers under a TEM microscope. For 3 months stability test, the formulations had no phase separation and gave the slightly changed values of particle size, polydispersity index (PDI), zeta potentials, and pH values. In addition, multiple nanoemulsions also enhanced the stability of active compounds, with the highest percentage of remaining content of curcumin and arbutin at 94.69 and 90.45 %, respectively at 4 °C for 3 months. In a cell culture test on $B_{16}F_{10}$, 2DS at 0.05 g/ml gave no cell cytotoxicity and anti-melanogenesis at 57.75 ± 5.74 %, the same potency as kojic acid at a concentration of 20 μg/ml. Therefore, this study will be useful to prepare multiple nanoemulsions for further development into novel health care products.

* Corresponding author. Department of Pharmaceutical Sciences, Faculty of Pharmacy, Chiang Mai University, Chiang Mai, 50200, Thailand.
E-mail address: mathukorn.s@cmu.ac.th (M. Sainakham).

https://doi.org/10.1016/j.heliyon.2024.e34665
Received 28 August 2023; Received in revised form 25 June 2024; Accepted 15 July 2024
Available online 15 July 2024

1. Introduction

Melanin is an essential pigment found in the skin that serves a critical function in protecting DNA from the harmful effects of UV rays, which have the potential to induce skin cancer. Melanin, despite its skin-protective properties, is also involved in melanoma and abnormal pigmentation [1]. Melanin overproduction can lead to considerable aesthetic distress and can disturb the individual concerned, particularly in instances of increased pigmentation such as melasma, solar age spots (lentigo), and facial freckles [2]. The process of skin pigmentation occurs in the skin, where melanocytes produce melanin, or pigment. When melanocytes are stimulated, tyrosinase, an enzyme that is activated by oxidation, sends sequential signals inside the cell [3,4]. This enzyme accelerates the conversion of l-tyrosine to 3,4-dihydroxyphenylalanine (l-dopa). The l-dopa is then oxidized into dopaquinone and further synthesized into melanin. There are two different types of melanin, eumelanin and pheomelanin. Eumelanin is a brown pigment synthesized by Tyrosinase-related protein 1 (TRP-1) and DOPAchrome tautomerase (DCT) or TRP-2, while pheomelanin is a yellow pigment synthesized by dopaquinone and cysteine or glutathione [5,6]. The pigmentation response has a strong relationship with tyrosinase activity. Tyrosinase is a protein containing copper in its active site, which accelerates the hydroxylation process and results in the development of various forms of skin pigmentation [7]. As a result, it is popular for cosmetic products to contain active compounds with properties that suppress tyrosinase activity in the melanin pigmentation process. Depending on the structure of the inhibitor, the inhibitory action of these compounds may be either competitive or non-competitive [8]. However, existing treatments for hyperpigmentation are accompanied by toxicity, poor skin penetration, instability, and/or ineffectiveness. As a result, transdermal delivery must be improved in order to properly administer active substances for topical applications [9]. Dosage formulations commonly utilized in cosmetics have a limited affinity for the skin and little penetration ability. Therefore, the desired impact cannot be achieved when conventional cosmetics are utilized as cosmeceuticals, as the active component is unable to reach the target site [10]. By effectively decreasing the size of active ingredients to the nanoscale and altering their characteristics, including permeability, water solubility and surface characteristics, nanotechnology has the potential to overcome the limitations associated with conventional dosage forms [11]. Nanoemulsions are a crucial technology that has the potential to drive new product innovations in the field of nanotechnology.

Nanoemulsions are currently one of the nanotechnologies receiving the most interest. The internal particle size ranges from 20 to 200 nm, constituting a thermodynamically unstable system that appears translucent or transparent due to its tiny particle size, thus reducing light scattering. Nanoemulsions appearance is dependent on particle size. If the particle size is below 100 nm, the product will seem translucent. Due to Brownian movement, particles larger than 100 nm have a milky appearance, while smaller particles also contribute to the kinetic stability of nanoemulsions [12,13]. Nanoemulsions, which are unstable systems, cannot be spontaneous during their preparation. It also requires a process of preparation that is performed by machine tools. There are two different preparation processes: high energy preparation and low energy preparation [14]. At present, there is a growing interest in the utilization of multiple nanoemulsions as an attractive vehicle to control the delivery of cosmetics and achieve complete penetration of lipophilic and hydrophilic active ingredients in specific skin layers through an increase in their concentration within the skin. The two primary design characteristics of multiple nanoemulsions that can be utilized for purposes unrelated to those of simple nanoemulsions are the internal morphology and the droplets' ability to solubilize both aqueous and organic substances. A significant proportion of multiple nanoemulsions are composed of a mixture of polar aqueous and nonpolar oil phases contained inside. This characteristic enables the co-encapsulation, co-localization, internal segregation, and/or release of hydrophobic and hydrophilic components, all of which are unattainable in single nanoemulsions. For now, the predominant application of co-solubilization of many nanoemulsions has been in the field of drug delivery [15].

In this study, the purpose was to develop a nanoemulsion including active compounds with a whitening effect. After loading the active compounds into both oil and water phases, the physicochemical properties, stability test, cell toxicity and anti-melanogenesis in cell culture were evaluated. The findings of this study will be beneficial for those interested in the development of novel health care and cosmetic products.

2. Material and methods

2.1. Materials

Dimethyl sulfoxide (DMSO), thiazolyl blue tetrazolium bromide (MTT), tyrosinase from mushroom, l-dopa, l-tyrosine were obtained from Sigma Chemicals Co., St. Louis, MO, USA. Span 60 (HLB = 4.7), Tween 60 (HLB = 14.9), Span 80 (HLB = 4.3) and Tween 80 (HLB = 15.0) were all acquired from Namsiang Co. Ltd., Thailand. Glycerin, sunflower oil, olive oil, isododecane and isopropyl myristate (IPM) were from Union Science, Thailand. Polyglyceryl-3 polyricinoleate (PGPR, HLB = 4.0), oil-soluble thickener (Sugar gel), alpha arbutin and curcumin were from Chanjao Longevity Co., Ltd., Thailand. The completed DMEM medium mixed with 10 % fetal bovine serum, 100 U/ml penicillin and 100 mg/ml streptomycin was from GIBCO, Invitrogen 95 Corporation, NY, USA. All the remaining chemicals and reagents were of analytical grade.

2.2. Tyrosinase inhibitory activity

Tyrosinase inhibitory activity was determined according to the method of a previous study with modifications [16]. Mixed a 20 μl sample (0.2–2,000 μM) with 40 μl phosphate buffer pH 6.8 at a concentration of 0.1 M, 20 μl tyrosinase solution in each well of a 96-well plate, and incubate at room temperature for 10 min. At the end of the time, a substrate solution of 20 μl l-dopa or l-tyrosine was

added, mixed well, incubated at room temperature for 10 min, and then the absorbance was measured at 475 nm with a microplate reader. At the end of the time, a substrate solution of 20 μl l-dopa or l-tyrosine was added, mixed well, incubated at room temperature for 10 min, and then the absorbance was measured at 475 nm with a microplate reader. The measured value in each concentration was used to calculate % Tyrosinase inhibition as follows (Equation (1)):

$$\% \text{ Tyrosinase inhibition} = [(A_{control} - A_{sample})/ A_{control}] \times 100 \quad (1)$$

$A_{control}$ was the control group absorbance, and A_{sample} was the treated sample absorbance. The percentage of tyrosinase inhibition and sample concentration were then used to generate a standard curve of IC_{50} value, which was the concentration of the sample that caused tyrosinase inhibition activity at 50 %. Then, using the following formula, examined the relationship between the samples by using the combination index (CI) as follows (Equation (2)):

$$CI = (IC_{50amix} / IC_{50a}) + (IC_{50bmix} / IC_{50b}) \quad (2)$$

IC_{50a} and IC_{50b} were the concentrations of the single substance that induced 50 % tyrosinase inhibition, whereas IC_{50amix} and IC_{50bmix} were the concentrations of each single substance in a combination that causes 50 % tyrosinase inhibition. The calculated CI value may be less than or more than 1 implying additive, synergistic or antagonistic interactions in the combination, respectively [17].

2.3. Emulsion preparation

2.3.1. Preparation of W/O/W emulsions by low energy method

Using the one-step emulsification process, 50 g of W/O/W emulsions were prepared with modifications [18]. The use of surfactant mixtures was in accordance with Table 1. The overall concentration of surfactants was kept at 5 % (w/w). In the oil phase, both surfactants were dissolved. The oil and 35 g of water phases using distilled water were independently heated to 70 ± 5 °C. To improve mixing conditions, the water phase was gently added to the oil phase while stirring at 500 rpm (Mechanical Agitator-ST1, Heidolph, Germany) until the temperature reached room temperature. The optimal formulations with a homogeneous distribution of the emulsion components were chosen to load the active ingredients as follows: 0.3 % (w/w) alpha-arbutin in the aqueous phase and 1 % (w/w) curcumin in the oil phase.

2.3.2. Preparation of W/O/W emulsions by high energy method using ultrasonication

The formulations were prepared as described previously with some modifications to generate W/O coarse emulsion as W/O/W nanoemulsion with components in Table 2 [19]. To produce the W/O/W multiple nanoemulsion, the optimal ultrasonication conditions utilizing a probe sonicator (JY96-IIN, Scientz, Ningbo, China) were 180 s in a pulse mode (60 s on and 60 s off) at 20 kHz with 40 % amplitude. The water phase in 50 g of W/O/W nanoemulsions was 1 g internal phase and 39.5 g external phase. The formulations were kept at room temperature for 24 h to examine phase separation before selecting the optimal formulations to load the active components as previously described.

2.4. Physicochemical characteristic examination of formulation

Particle size, PDI value and zeta potential of the formulation were determined by a dynamic laser light scattering analyzer (SZ-100; Horiba Scientific, Japan) following the method described with modifications [20]. Each loaded nanoemulsion was diluted with deionized water by 1,000 folds to avoid multiple scatterings. The preliminary investigations of pH and morphology were examined by pH indicator strips (Merck, Darmstadt, Germany) at room temperature and a light microscope (CH-2, Olympus, Japan), respectively. The microstructure of nanoemulsion was studied using TEM (JEM-2010, JEOL, Japan) according to the prior approach [21].

2.5. Cytotoxicity assay by MTT assay

Toxicity test in cell cultures was performed using MTT analysis with modifications [22]. Murine melanomas, or $B_{16}F_{10}$ cells, were obtained from American Type Culture Collection (ATCC) (Virginia, USA) and cultured in DMEM with 10 % fetal bovine serum in

Table 1
The ingredients of multiple emulsions prepared by low energy method.

Sample	Emulsifier (g)				Oil (g)			
	Tween60	Tween80	Span60	Span80	Sunflower oil	Olive oil	Isododecane	Isopropyl myristate
1A	1.67	–	0.83	–	12.5	–	–	–
1B	1.67	–	0.83	–	–	12.5	–	–
1C	1.67	–	0.83	–	–	–	12.5	–
1D	1.67	–	0.83	–	–	–	–	12.5
2A	–	1.67	–	0.83	12.5	–	–	–
2B	–	1.67	–	0.83	–	12.5	–	–
2C	–	1.67	–	0.83	–	–	12.5	–
2D	–	1.67	–	0.83	–	–	–	12.5

Table 2
The ingredients of multiple nanoemulsions prepared by high energy method using ultrasonication.

Sample	Emulsifier (g)					Oil (g)				Thickener (g)	
	Tween 60	Tween 80	Span 60	Span 80	PGPR	Sunflower oil	Olive oil	Isododecane	Isopropyl myristate	Sugar gel	Glycerin
1A	0.5	–	0.5	–	–	8.5	–	–	–	–	–
1B	0.5	–	0.5	–	–	–	8.5	–	–	–	–
1C	0.5	–	0.5	–	–	–	–	8.5	–	–	–
1D	0.5	–	0.5	–	–	–	–	–	8.5	–	–
2A	–	0.5	–	0.5	–	8.5	–	–	–	–	–
2B	–	0.5	–	0.5	–	–	8.5	–	–	–	–
2C	–	0.5	–	0.5	–	–	–	8.5	–	–	–
2D	–	0.5	–	0.5	–	–	–	–	8.5	–	–
2DS	–	0.5	–	0.5		–	–	–	7.225	0.425	0.85
3B	–	0.5	–	–	0.5	–	8.5	–	–	–	–
3D	–	0.5	–	–	0.5	–	–	–	8.5	–	–
3DS	–	0.5	–	–	0.5	–	–	–	7.225	0.425	0.85

96-well plates and incubated in the CO_2 incubator for 24 h. At the end of the time, nanoemulsions at 0.5–0.00005 g/ml were added to the 96-well plates. Continue incubated for another 24 h, then washed off the medium, added MTT solution, and incubated again for 4 h. At the end of experiment, the dye was removed, dissolved in DMSO to measure absorbance, and calculated the percentage of cell viability (% Cell viability) according to the following Equation (3):

$$\% \text{ Cell viability} = [A560_{sample} / A560_{control}] \times 100 \quad (3)$$

$A560_{sample}$ was the absorbance value at a wavelength of 560 nm obtained from the group treated with the samples, and $A560_{control}$ was the absorbance value at a wavelength of 560 nm obtained from the group that was not treated with the samples. Sample concentrations resulting in % Cell viability greater than 70 % will be used for the next experiment [23].

2.6. Anti-melanogenesis activity on $B_{16}F_{10}$ murine melanomas

$B_{16}F_{10}$ cells were cultured in a 6-well plate and incubated in a CO_2 incubator for 24 h. Then, the sample was added to the appropriate concentration and incubated for another 72 h. At the end of the time, the cells were washed with 1xPBS, dissolved in 10 % NaOH and incubated at 60 °C for 1 h. The absorbance at 450 nm was used to measure the amount of melanin and calculate the inhibitory effect of melanin (% Anti-melanogenesis) as shown in the following Equation (4):

$$\% \text{ Anti-melanogenesis} = 100 - [(Mt / Mc) \times 100] \quad (4)$$

Mt was the melanin content of the group treated with the samples, and Mc was the melanin content of the control group that was not treated with the samples [23].

2.7. Stability test of formulation

After preparing and leaving at room temperature for 24 h, the stable nanoemulsions without phase separation were visually observed and selected to investigate their stability. For stability tests, the nanoemulsions were stored at 4, 25, and 45 °C for 3 months. The phase separation, pH, particle size, zeta potential, and PDI were determined as previously described. To determine the amount of curcumin and alpha-arbutin in the formulation, the samples were diluted with 95 % alcohol at a 1:10 ratio (v/v) and centrifuged at 5,000 rpm for 3 min at room temperature to collect the supernatant. The content of curcumin and alpha-arbutin was determined using a UV spectrophotometer by comparing the standard curve at absorbances of 425 and 285 nm, respectively [24,25]. The active content in nanoemulsions was expressed as the percentage of remaining active content at observing time per active content at initial time as previously described [20].

2.8. Data analysis

All assays were performed in triplicate in three independent separate experiments. The data was presented as mean ± SD (standard deviation). The results were evaluated using one-way analysis of variance (ANOVA) with significance levels of $p < 0.05$ and $p < 0.01$ in SPSS version 17 (IBM Corporation, Armonk, NY).

3. Results and discussion

3.1. Tyrosinase inhibitory activity test

Tyrosinase is a copper-containing metalloenzyme that is common in nature, ranging from microbes to plants to humans. Following

oxidation to quinones, it accelerates the o-hydroxylation of monophenols into catechols. Its physiological role is to convert l-tyrosine into dopaquinone, which is required for melanin production in melanosomes. l-tyrosine or phosphorylated isomers of l-3,4-dihydroxyphenylalanine (l-dopa) function are crucial molecules in the control of melanin production [26]. In this research, the tyrosinase inhibitory activity using l-tyrosine and l-dopa as substrates to produce *in vitro* melanin production was determined by active compounds from kojic acid dipalmitate and curcumin as oil-soluble substances, and alpha arbutin and magnesium ascorbyl phosphate as water-soluble substances. It was found that magnesium ascorbyl phosphate had the highest tyrosinase inhibition at an IC_{50} value of 78.99 ± 5.86 μM when tested with l-dopa as a substrate, while curcumin had the highest tyrosinase inhibition at an IC_{50} value of 39.64 ± 5.76 μM when tested with l-tyrosine, as shown in Table 3. Previous studies indicated that when melanocytes were treated with 1 mM magnesium ascorbyl phosphate for 48 h, no noticeable cytotoxic or cell growth inhibiting effects were observed. However, the tyrosinase activity and melanin concentration of melanocytes were markedly reduced in a dose-dependent manner [27]. Additionally, curcumin inhibited tyrosinase activity and decreased melanin content dose-dependently, without affecting melanocyte viability, at doses between 1.25 and 10 μM. Curcumin-treated human melanocytes demonstrated dose-dependent downregulation of melanogenesis-related proteins (microphthalmia-associated transcription factor (MITF) signaling on expression of tyrosinase, tyrosinase-related proteins 1 and 2 (TRP-1, TRP-2) [28]. According to these results, most oil-soluble substances had IC_{50} values greater than 2000 μM, and most of the active substances tested with l-tyrosine had a low IC_{50} value. Therefore, the synergistic effect of the tyrosinase inhibition study used l-tyrosine as a substrate and selected these active compounds to be prepared as mixtures between oil-soluble compounds and water-soluble compounds in a ratio of 1:1. In previous studies, the prepared solutions were used in bioactivity assays in a ratio of 1:1 to observe the interaction properties of the mixtures. Resveratrol and other phenolic compounds in red wine have been reported to be responsible for positive and promising health benefits from antioxidant activity [29]. The results of the tyrosinase inhibition activity investigation also revealed an approach for combining antioxidants and tyrosinase inhibitors in a ratio of 1:1 that exhibited a synergistic inhibitory impact on tyrosinase activity, which is beneficial for the treatment of skin disorders [17]. In Table 4, it was found that the mixture of curcumin and alpha arbutin had the highest tyrosinase inhibition with an IC_{50} value of 63.58 ± 4.99 μM and a CI value of 0.99, which meant that this mixture had a synergistic action on tyrosinase inhibition activity. However, mixtures containing kojic acid dipalmitate were not be selected because a single compound with an IC_{50} value greater than 2000 μM which had weak inhibition of tyrosinase activity. The phenolic compound, namely curcumin, had been isolated from the methanolic plant extract and showed potent tyrosinase inhibitory activities via competitive enzyme inhibition. 4-hydroxyl groups in the phenolic rings of curcumin analogs made them potent inhibitors of tyrosinase activity [30]. In research of alpha-arbutin on tyrosinase inhibitory activity, it was shown that alpha-arbutin had the potential to suppress melanin synthesis in human melanoma cells without inducing cytotoxicity in human skin [31]. Additionally, the anti-tyrosinase activity of the combination of aloesin and arbutin was studied. They demonstrated that combination treatment was much more successful in the synergistic inhibitory mechanism of tyrosinase in pigmentation reduction at 63.3 % in treating hyperpigmentation disorders than aloesin and arbutin alone at 34 and 43.5 %, respectively [32]. Scientists are now investigating natural substances that have a synergistic impact on tyrosinase inhibition. The suppression of tyrosinase includes the overall phenol oxidation process in the synthesis of melanin. Previous findings demonstrated that the synergistic impact on tyrosinase activity induced by two substances was significantly decreased by the synergistic interaction between natural antioxidants and potent tyrosinase inhibitors [17]. Thus, alpha-arbutin and curcumin were selected as active compounds to be developed into nanoemulsions.

3.2. Evaluation of physicochemical characteristic formulation

According to the previous study on nanoemulsion preparation, there were two methods: low energy and high energy. After 1 week of storage, the best formulation was determined. The formulation was selected for further preparation based on the absence of phase separation. To incorporate the active compounds into the formulation for a low energy preparation, 2C and 2D were chosen because they did not undergo phase separation after 24 h. However, 2C and 2D containing active compounds exhibited phase separation after kept for 24 h. The surface free energy is raised when the dispersed phase of multiple emulsions is broken down into droplets. The increase in interfacial free energy results in the thermodynamic instability of the dispersed phase, which leads to droplet coalescence and phase separation. For example, a W/O/W emulsion contains both water-in-oil and oil-in-water-type emulsions, requiring the presence of at least two emulsifiers: one that is predominately hydrophobic, stabilizing the primary W/O emulsion, and one that is predominately hydrophilic, stabilizing the secondary O/W emulsion [33]. The type and concentration of Span have been mentioned as critical stability parameters for Span/Tween-stabilized multiple emulsions [34]. Although the low energy method may not be appropriate for emulsion preparation from the ingredients in this study, it could be used to select preliminary components from formulations that may be appropriate for the next formulation. In high energy preparation, the blank formulations (2B, 2C, and 2D)

Table 3
The IC_{50} value of tyrosinase inhibitory effects of single compound with l-dopa or l-tyrosine as a substrate.

Code	Sample	IC_{50} (μM)	
		l-dopa	l-tyrosine
KAD	Kojic acid dipalmitate	>2000	>2000
AA	Alpha arbutin	>2000	165.99 ± 7.38
CC	Curcumin	>2000	39.64 ± 5.76
MAP	Magnesium ascorbyl phosphate	78.99 ± 5.86	245.91 ± 34.66

Table 4
IC_{50} value and CI value of mixtures with L-tyrosine as a substrate.

Sample	IC_{50} comparison	IC_{50} (μM)	CI value
KAD + AA	KAD > AA	587.09 ± 213.93	–
KAD + MAP	KAD > MAP	>2000	–
CC + AA	CC < AA	63.58 ± 4.99	0.99 (synergistic)
CC + MAP	CC < MAP	88.55 ± 15.50	1.3 (antagonistic)

Note: CI values equal, smaller, or greater than 1 indicate an additive, synergistic, or antagonistic effect, respectively.

with no phase separation after storage for 24 h would be used. Only the 2B and 2D loadings the active compounds could preserve good dispersibility after 24 h. The total amount of surfactants in 2B and 2D was kept at 1.0 % (w/w) resulting in mixed HLB values of Tween 80 and Span 80 of 9.7. The high energy emulsification procedure has been utilized to produce multiple nanoemulsions. By selecting appropriate surfactants, it is possible to produce the primary nanoemulsion. For instance, a lipophilic surfactant with a low HLB value could be used. A W/O/W nanoemulsion can be produced by emulsifying this emulsion with an outer phase containing a hydrophilic surfactant with a high HLB value using a high energy mixer apparatus. However, the analysis showed significant multiple droplets for each of the composition factors examined. This observation implies that the formation of multiple nanoemulsions may be affected by several formulation parameters, not only the HLB values but also the ratios of emulsion compounds in oil and water [18]. In the subsequent experiment, these formulations were improved by adding a thickening agent and altering the emulsifying agent to increase their stability and obtain 2DS and 3DS loadings of active compounds without phase separation after storage for 24 h. The oil-based thickener could retain and protect internal water droplets within the oil phase by establishing a stable and strong network within the oil globules, resulting in enhanced oil-water interphase stability. In addition, the thickener solubilized in oil improved the viscosity of the oil phase and increased stability by co-interaction with oil-soluble surfactants at the water-oil interphase which is the key to the production of the lowest mean droplet diameter and dispersity index [19]. Therefore, 2B, 2D, 2DS, and 3DS, which indicated good stability, were chosen to further examine the characteristics of the formulation as shown in Fig. 1. The selected formulations with no phase separation from previous preparations were evaluated for their physicochemical characteristics as shown in Table 5. The particle size, PDI value and zeta potential gave values in the range of 225.63–1196.00 nm, 0.122 to 1.198 and −79.83 to −62.13 mV, respectively. 2D tended to have particle sizes outside the nanoparticle range (>1,000 nm) with a significant difference at $p < 0.05$ compared to other formulations. 2DS and 3DS showed a significant difference in their low PDI values compared to other formulations at $p < 0.05$. Moreover, 2DS also showed the lowest zeta potential at −79.83 ± 2.23 mV ($p < 0.05$) in this preparation. Therefore, only 2B, 2DS and 3DS were selected for further studies. The properties of the formulation such as pH, morphology observation by light microscope and transmission electron microscope (TEM) were examined. The pH values of nanoemulsions from 2B, 2DS and 3DS were 6.5, 5.5 and 4.5, respectively, which were close to the pH of the skin of a healthy human. Skin surface pH characterizes the pH environment on the skin and, as a result, whether the lipid-processing enzymes are functioning within the optimal acidic pH range required to produce the lipid matrix. The ideal pH range for healthy skin is between 4.5 and 5.9, but this range may differ between males and females because the effect of gender is still unclear [35]. The examination of formulation appearance under a light microscope and transmission electron microscope (TEM) was shown in Fig. 2. The internal particles in each formulation had a spherical

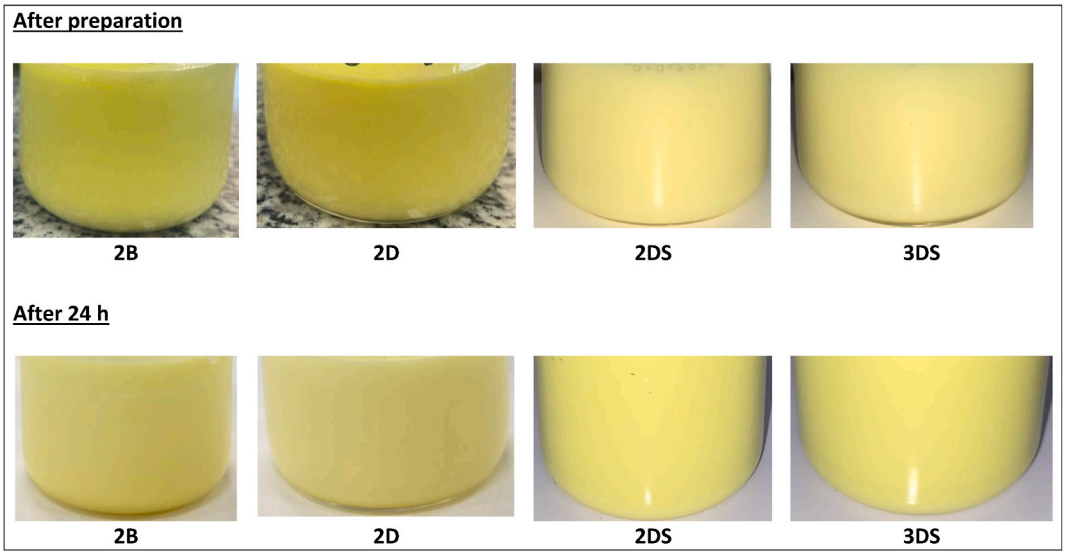

Fig. 1. Appearance with no phase separation of 2B, 2D, 2DS and 3DS nanoemulsions prepared by high energy method using ultrasonication after preparation and kept for 24 h.

Table 5
Particle size, PDI value, zeta potential, and pH value of the selected nanoemulsion after kept for 24 h.

Sample	Particle size (nm)	PDI value	Zeta potential (mV)	pH
2B	409.50 ± 9.05^{a}	0.453 ± 0.073^{a}	-62.13 ± 1.01^{a}	6.5
2D	1196.00 ± 308.00^{b}	1.198 ± 0.081^{b}	-78.3 ± 2.2^{b}	–
2DS	225.63 ± 5.69^{c}	0.199 ± 0.099^{c}	-79.83 ± 2.23^{b}	5.5
3DS	277.07 ± 5.97^{d}	0.122 ± 0.047^{c}	-64.53 ± 1.25^{a}	4.5

Note: Differences in alphabets (a, b, c, and d) imply significant differences ($p < 0.05$) between the formulation.

shape and varied sizes, which were comparable to the particle sizes previously determined using a particle analyzer. It was revealed that 2B had the largest internal particle size, whereas 2DS and 3DS had internal particle sizes that were fairly similar.

3.3. Cytotoxicity test in $B_{16}F_{10}$ cells

A murine malanoma cell line, or $B_{16}F_{10}$, which produced a high amount of melanin pigment and rapid growth, was investigated at an appropriately high concentration without cytotoxicity and provided greater than 70 % cell viability relative to the control in the cytotoxicity test. Consequently, the data should demonstrate that the decrease in melanin content was not caused by cell death [23]. According to the safety of nanoemulsions, the results showed that some samples showed toxicity in cell lines with a percentage of cell viability below 70 % at a maximum concentration of 0.5 g/ml, which affected the production of melanin in cell lines. Hence, all samples prepared at a lower concentration of 0.05 g/ml found that they had a percentage of cell viability greater than 70 %, while the control group that did not receive any substance had a percentage of 101.12 ± 2.63 % as shown in Table 6. The varied cytotoxic effects of the samples may be attributable to the distinct cell types that respond differently to a certain compound [36]. According to a prior investigation, $B_{16}F_{10}$ cell line was not cytotoxic to the hull and seed extracts of Bambara groundnut at concentrations of 0.1 mg/ml, as they gave more than 70 % cell viability in comparison to the control group. Nevertheless, the extracts at a concentration of 1 mg/ml are regarded as minimally cytotoxic to $B_{16}F_{10}$ cells [23]. In this study, the concentration of 0.05 g/ml was considered safe for the $B_{16}F_{10}$ cell line in further experiment.

3.4. Melanin production inhibition assay in $B_{16}F_{10}$ cells

Melanin production is the process of preventing harmful sunlight from the environment, which damages the skin. Additionally, it protects the skin from damage caused by UV radiation. However, excessive melanin production can result in skin conditions such as freckles, melasma and melanoma [5]. In this study, $B_{16}F_{10}$ cells mimicked the *in vitro* pigmentation process. After 72 h of testing on cell cultures, it was found that the control group that did not receive any substances, 2B and 2B blank (2Bb) had no effect on melanin production inhibition (data not shown), while 2DS, 2DS blank (2DSb), 3DS and 3DS blank (3DSb) had the effect of melanin production inhibition as shown in Fig. 3. Kojic acid is a well-known inhibitor of tyrosinase. When l-dopa, norepinephrine and dopamine are oxidized by tyrosinase, kojic acid efficiently decreases the rate of pigment production [37–39]. Most *in vitro* and $B_{16}F_{10}$ cell culture screenings for novel tyrosinase inhibitors included common whitening agents, such as kojic acid, as positive controls in the experiments [40,41]. In this study, kojic acid used as a standard agent at a concentration of 20 μg/ml had a percentage of anti-melanogenesis activity of 44.54 ± 2.47 %, while 2DS and 3DS formulations containing the active compounds were 57.75 ± 5.74 and 73.31 ± 4.39 %, respectively, with a higher significant difference than kojic acid and their blank formulation at $p < 0.01$. Curcumin is commonly regarded as having positive effects on human health; however, its insolubility and stability represent considerable challenges to the reliable use of its therapeutic effects. $B_{16}F_{10}$ cells stimulated with α-MSH exhibited a reduction in both cellular melanin concentration and tyrosinase activity when treated with curcumin. Curcumin inhibited the production of proteins associated with melanogenesis in $B_{16}F_{10}$ cells stimulated with α-MSH including microphthalmia-associated transcription factor (MITF), tyrosinase and tyrosinase-related proteins 1 and 2. Curcumin triggered melanogenesis-regulating signals including mitogen-activated protein kinase kinase (MEK)/extracellular signal-regulated kinase (ERK) or phosphatidylinositol 3- kinase (PI3K)/Akt in $B_{16}F_{10}$ cells treated with or without α-MSH. By way of PD98059 and LY294002, the inhibitory action of curcumin on α-MSH-induced melanogenesis was diminished. In summary, inhibitory effect of curcumin on melanogenesis triggered by α-MSH may be achieved by inhibiting MITF and its subsequent signaling cascade via activation of MEK/ERK or PI3K/Akt [42]. Essential and effective measures to prevent the production of melanin include inhibiting tyrosinase activity. The inhibitory potency of a potentially effective inhibitor may be assessed using positive controls. Changing test parameters, including substrate concentrations, incubation times, and tyrosinase sources, pose significant challenges in terms of exerting an influence. Arbutin is a well-known depigmenting agent and tyrosinase inhibitor. For the purpose of screening new components or extracts that suppress melanin synthesis, they are widely utilized as positive controls [41]. In cell culture tests, it is believed that the increase in cell survival induced by arbutin results from an endogenous decrease in the catalytic activity of $B_{16}F_{10}$ cellular tyrosinase within cells, subsequently leading to a reduction in melanin concentration. A study reported that 0.25–0.5 mM alpha-arbutin decreased melanin content and tyrosinase activity in a dose-dependent manner, although 0.25–1 mM alpha-arbutin had no effect on cell proliferation in cultured human melanoma cells [43]. In addition, it has been found that aliphatic esters, such as isopropyl myristate (IPM), cause disordering effects on the rigid stratum corneum lipid membranes and are frequently used as penetration enhancers in various cutaneous formulations. IPM will mainly affect the lipids of the stratum corneum and enhance the diffusivity and/or partition coefficient of drugs. Although IPM is a lipophilic molecule, its ester group contains a minor polar

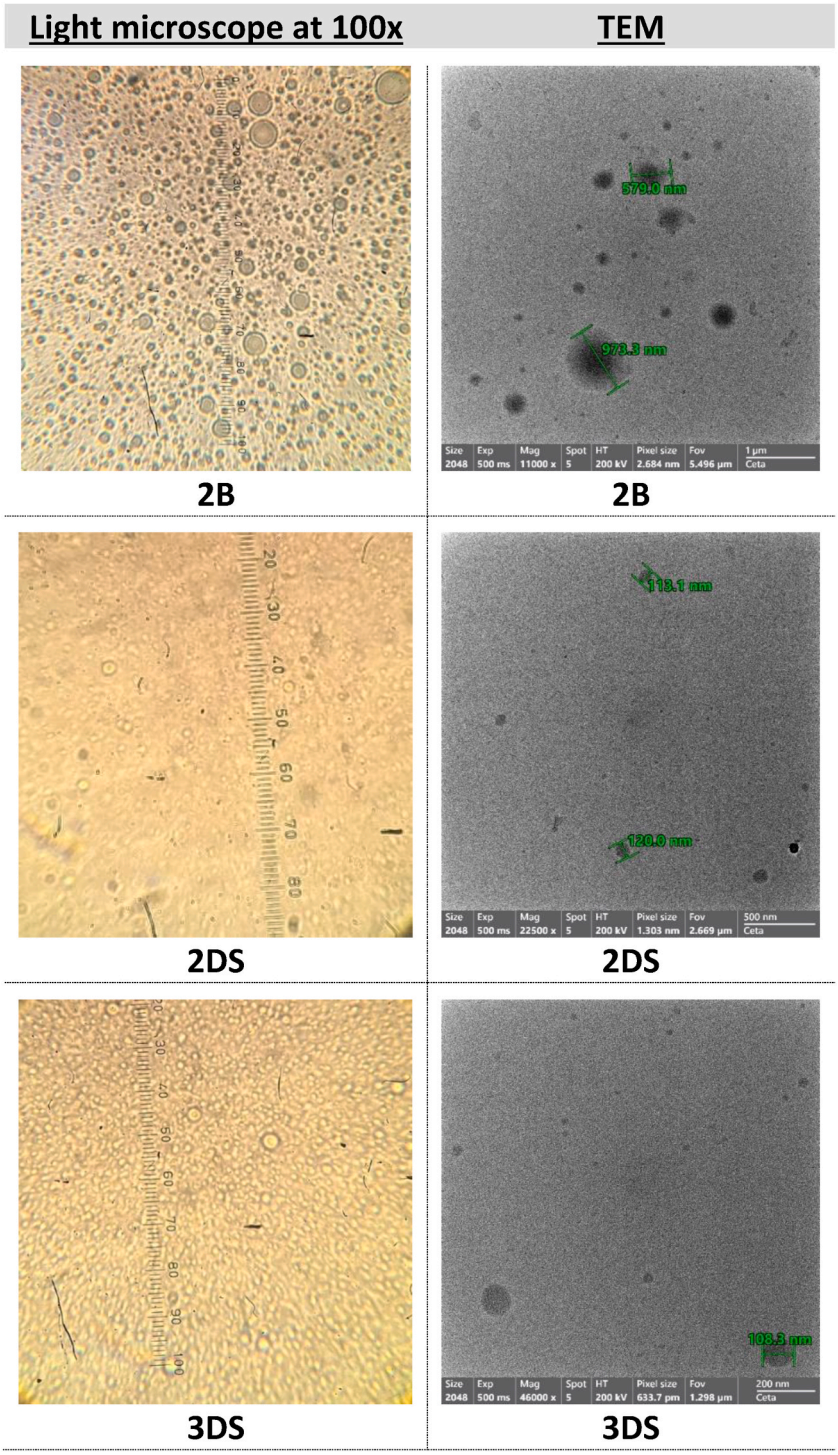

Fig. 2. The examination of preliminary appearance by light microscope, and microstructure morphology by transmission electron microscope (TEM) of 2B, 2DS and 3DS nanoemulsions kept for 24 h.

moiety. It lacks a distinct head-to-tail polarity, which is advantageous for its interaction with membranes [44]. In prior experiments, this nano-structured emulsion formulation containing IPM enhanced the skin penetration of several active compounds. Isopropyl myristate in drug-loaded microemulsions increased the permeation of temozolomide acid hexyl ester through rat skin, resulting in less drug retention in the skin [45], whereas resveratrol-loaded nanoemulsions containing IPM and low amounts of Tween80/Span demonstrated the greatest permeation ability [46]. Inhibition of tyrosinase may be enhanced by formulations loaded with active

Table 6
The percentage of cell viability of the selected nanoemulsions in $B_{16}F_{10}$ cells.

Conc. (g/ml)	%Cell viability						
	2B	2B blank	2Ds	2Ds blank	3Ds	3Ds blank	Control
0.00005	105.34 ± 1.91	118.65 ± 8.97	158.35 ± 13.85	101.33 ± 1.43	111.25 ± 2.82	103.95 ± 5.23	101.12 ± 2.63
0.0005	112.92 ± 2.59	113.90 ± 9.29	138.24 ± 5.18	116.19 ± 6.25	106.20 ± 2.08	108.13 ± 5.42	
0.005	109.92 ± 3.92	86.66 ± 5.30	115.64 ± 6.27	114.26 ± 4.96	98.99 ± 4.40	105.38 ± 7.45	
0.05	93.60 ± 2.38	74.77 ± 3.23	122.06 ± 6.42	112.69 ± 4.91	79.57 ± 10.52	94.08 ± 6.01	
0.5	77.54 ± 3.38	65.18 ± 1.09	91.19 ± 0.66	113.14 ± 2.38	41.09 ± 1.11	68.21 ± 2.01	

Note: blank = nanoemulsion without curcumin and alpha-arbutin.

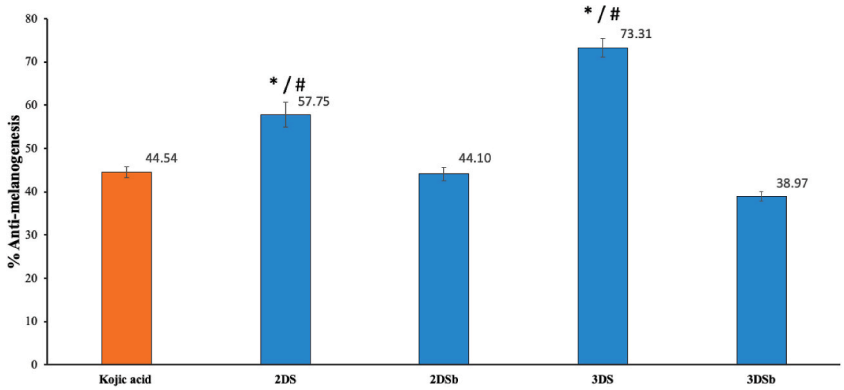

Fig. 3. The percentage of anti-melanogenesis activity in B16F10 cells treated by nanoemulsions and kojic acid at the concentration of 0.05 g/ml and 20 μg/ml, respectively. The asterisk (*) indicated significant difference compared with kojic acid ($p < 0.01$); The hash mark (#) indicated significant difference compared with their blank formulation ($p < 0.01$).

compounds mixed with IPM, as indicated by these studies. Therefore, multiple nanoemulsions containing IPM, curcumin, and arbutin can contribute to being effective on pigmentation inhibition in this study.

3.5. *The physicochemical characteristics in stability test*

For stability studies, the nanoemulsions were kept at 4, 25, and 45 °C for 3 months. The pH, phase separation, particle size, particle size distribution, zeta potential and remaining active content were determined. The visual observations of all selected nanoemulsions showed good dispersibility at all temperatures for 1 month. In Figs. 4, 5 and 2B and 3DS stored at 4 ± 2, 25 ± 2 and 45 ± 2 °C and 2DS stored at 45 ± 2 °C for 2 months, resulted in phase separation. Moreover, 2B at 45 ± 2 °C after 7 days showed an obvious change in color from yellow to white as shown in Fig. 4. Curcumin has a pH-dependent color change. Under basic circumstances, the color change of curcumin is caused by the formation of phenoxide anion from the reaction of a phenolic hydroxyl groups with hydroxyl ions [47]. Curcumin's melting point is 183 °C. Nevertheless, curcumin undergoes hydrolytic breakdown at high temperatures. The rapid decrease

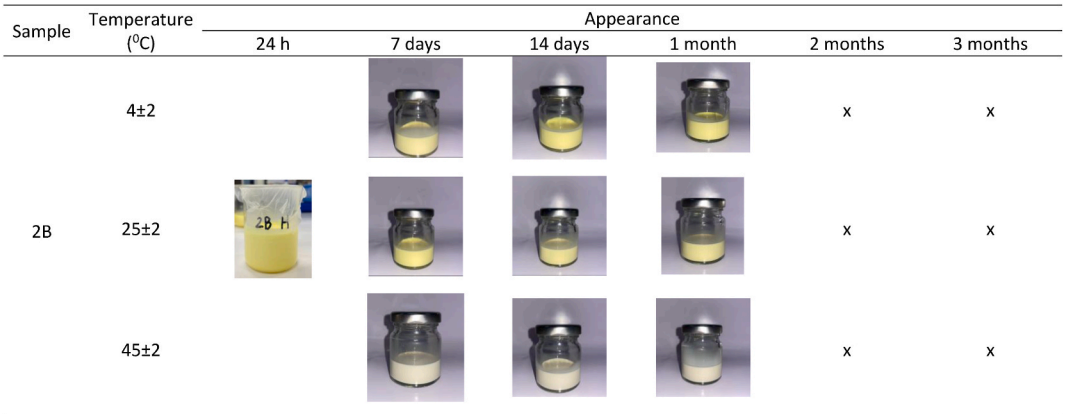

Fig. 4. Appearance of 2B nanoemulsion kept for 3 months at various temperatures; x = no investigate because of phase separation in nanoemulsion.

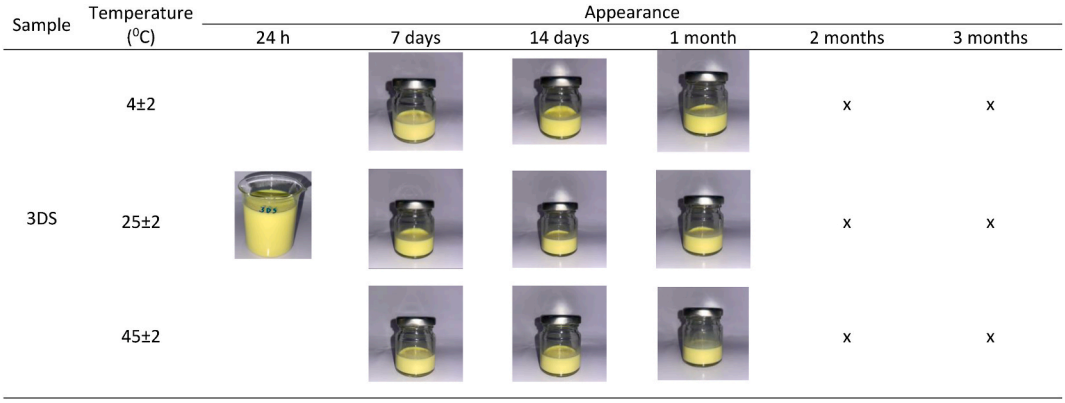

Fig. 5. Appearance of 3DS nanoemulsion kept for 3 months at various temperatures; x = no investigate because of phase separation in nanoemulsion.

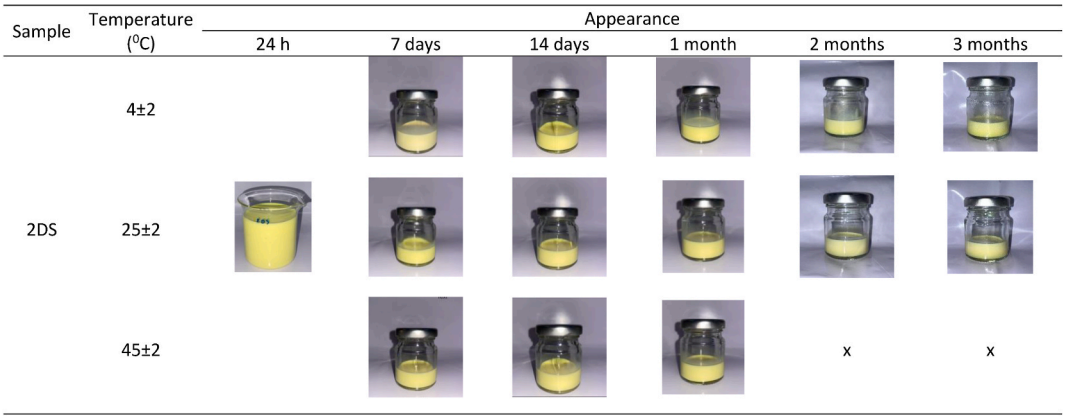

Fig. 6. Appearance of 2DS nanoemulsion kept for 3 months at various temperatures; x = no investigate because of phase separation in nanoemulsion.

Table 7
pH value of nanoemulsions kept for 3 months.

Sample	Temperature (^{0}C)	pH value					
		24 h	7 days	14 days	1 month	2 months	3 months
2B	4 ± 2	6.5	6.5	6.5	6.5	x	x
	25 ± 2		6.5	6.5	6.5	x	x
	45 ± 2		6.5	6.5	6.5	x	x
2DS	4 ± 2	5.5	5.5	5.5	5.5	5.5	5.5
	25 ± 2		5.5	5.5	5.5	5.5	5.5
	45 ± 2		5.5	5.5	5.5	x	x
3DS	4 ± 2	4.5	4.5	4.5	4.5	x	x
	25 ± 2		4.5	4.5	4.5	x	x
	45 ± 2		4.5	4.5	4.5	x	x

Note: x = no investigate because of phase separation in nanoemulsion.

in curcumin content with increasing temperature demonstrates its instability at high temperatures [48]. At the end of the study (3 months), 2DS maintained good stability in dispersibility and color when stored at 4 ± 2, and 25 ± 2 °C (Fig. 6). From the beginning of the examination at all temperatures, 2B, 2DS and 3DS had good pH stability with constant values of 6.5, 5.5 and 4.5 respectively. The 2DS with no phase separation was further examined in the next 2 and 3 months as shown in Table 7 and still had a stable pH of 5.5. In Tables 8 and 2B, 2DS and 3DS had particle sizes at the beginning of 409.50 ± 9.05, 225.63 ± 5.69 and 277.07 ± 5.97 nm, respectively. 2B and 3DS after kept for 1 month significantly increased ($p < 0.05$) the particle size at all temperatures. For 3 months storage of 2DS, the particle size kept in 4 ± 2 °C was 219.37 ± 8.50 nm which was similar to the beginning value, while the particle size kept at 25 ± 2 °C was 212.90 ± 0.40 nm with a significant difference at $p < 0.05$. At increasing temperatures, the instability of the droplets to

Table 8
Particle size of nanoemulsions kept for 3 months.

Sample	Temperature (^{0}C)	Particle size (nm)					
		24 h	7 days	14 days	1 month	2 months	3 months
2B	4 ± 2	409.50 ± 9.05	596.40 ± 25.64	659.88 ± 13.91	673.07 ± 11.45*	x	x
	25 ± 2		728.30 ± 11.61	700.13 ± 6.25	876.85 ± 37.55*	x	x
	45 ± 2		613.73 ± 30.58	950.65 ± 68.66	988.15 ± 16.33*	x	x
2DS	4 ± 2	225.63 ± 5.69	443.60 ± 60.67	185.63 ± 3.47	222.23 ± 3.61	247.57 ± 6.35	219.37 ± 8.50^{a}
	25 ± 2		224.37 ± 5.20	205.53 ± 13.58	210.01 ± 0.96	280.97 ± 6.25	212.90 ± 0.40^{a,*}
	45 ± 2		209.57 ± 6.43	950.83 ± 25.41	237.90 ± 6.08	x	x
3DS	4 ± 2	277.07 ± 5.97	275.50 ± 1.15	339.73 ± 9.37	1286.30 ± 0.85*	x	x
	25 ± 2		337.05 ± 15.63	291.85 ± 14.61	293.63 ± 6.55*	x	x
	45 ± 2		248.97 ± 8.30	611.07 ± 13.88	292.47 ± 11.67*	x	x

Note: x = no investigate because of phase separation in nanoemulsion; The asterisk (*) indicated significant difference compared with their formulation after kept for 24 h ($p < 0.05$); Similarity in alphabets imply no significant differences ($p < 0.05$) between the formulations.

Table 9
PDI value of nanoemulsions kept for 3 months.

Sample	Temperature (^{0}C)	PDI value					
		24 h	7 days	14 days	1 month	2 months	3 months
2B	4 ± 2	0.453 ± 0.073	0.447 ± 0.025	0.693 ± 0.016	0.817 ± 0.013*	x	x
	25 ± 2		1.024 ± 0.592	0.991 ± 0.005	0.522 ± 0.043	x	x
	45 ± 2		0.433 ± 0.046	2.331 ± 1.436	1.567 ± 0.114*	x	x
2DS	4 ± 2	0.199 ± 0.099	0.310 ± 0.017	0.332 ± 0.023	0.318 ± 0.313	0.394 ± 0.019	0.451 ± 0.064^{a,*}
	25 ± 2		0.493 ± 0.052	0.363 ± 0.107	0.231 ± 0.057	0.444 ± 0.023	0.418 ± 0.007^{a,*}
	45 ± 2		0.460 ± 0.007	3.283 ± 0.159	0.134 ± 0.098	x	x
3DS	4 ± 2	0.122 ± 0.047	0.612 ± 0.013	0.417 ± 0.024	2.488 ± 0.044*	x	x
	25 ± 2		0.646 ± 0.132	0.454 ± 0.043	0.378 ± 0.042*	x	x
	45 ± 2		0.540 ± 0.049	2.417 ± 0.136	0.295 ± 0.04*	x	x

Note: x = no investigate because of phase separation in nanoemulsion; The asterisk (*) indicated significant difference compared with their formulation after kept for 24 h ($p < 0.05$); Similarity in alphabets imply no significant differences ($p < 0.05$) between the formulations.

Table 10
Zeta potential of nanoemulsions kept for 3 months.

Sample	Temperature (^{0}C)	Zeta potential (mV)					
		24 h	7 days	14 days	1 month	2 months	3 months
2B	4 ± 2	−62.13 ± 1.01	−63.37 ± 1.33	−67.13 ± 1.47	−59.43 ± 1.72	x	x
	25 ± 2		−84.17 ± 2.71	−58.32 ± 1.01	−73.52 ± 3.21*	x	x
	45 ± 2		−48.17 ± 3.04	−53.33 ± 2.32	−74.27 ± 0.81*	x	x
2DS	4 ± 2	−79.83 ± 2.23	−71.97 ± 1.24	−45.11 ± 0.82	−63.91 ± 1.82	−68.71 ± 0.35	−63.83 ± 1.79^{a,*}
	25 ± 2		−82.87 ± 2.89	−47.67 ± 4.38	−73.22 ± 1.42	−70.93 ± 1.11	−58.93 ± 0.23^{b,*}
	45 ± 2		−71.87 ± 1.75	−63.53 ± 0.45	−77.17 ± 4.65	x	x
3DS	4 ± 2	−64.53 ± 1.25	−71.01 ± 3.03	−58.37 ± 0.61	−61.23 ± 2.74	x	x
	25 ± 2		−64.31 ± 1.73	−76.23 ± 2.03	−75.51 ± 3.72*	x	x
	45 ± 2		−63.41 ± 2.18	−45.42 ± 0.11	−65.57 ± 2.67	x	x

Note: x = no investigate because of phase separation in nanoemulsion; The asterisk (*) indicated significant difference compared with their formulation after kept for 24 h ($p < 0.05$); Differences in alphabets (a and b) imply significant differences ($p < 0.05$) between the formulations.

coalesce leads to an increase in mean particle diameter and phase separation. At elevated temperatures, dehydration of the non-ionic surfactant head group is responsible for the stability of nanoemulsions. Dehydration of the head group changes the optimal curvature of the surfactant monolayer and the solubility of the surfactant in the oil and water phases [49]. Previous research determined that nanoemulsions were physically stable to droplet growth at ambient temperatures with less than a 10 % change in diameter but were sensitive to droplet growth when subjected to elevated temperatures greater than 80 °C for 1 month of storage [50]. 2B, 2DS and 3DS had PDI values at the beginning of 0.453 ± 0.073, 0.199 ± 0.099 and 0.122 ± 0.047, respectively as shown in Table 9. 2B and 3DS after being kept for 1 month tended to increase the PDI values at all temperatures. The PDI value of 2DS kept for 3 months in 4 ± 2 and 25 ± 2 °C compared to the beginning value was significantly increased ($p < 0.05$) to 0.451 ± 0.064 and 0.418 ± 0.007, respectively. Table 10 showed the zeta potential of the formulations after storage at 4 ± 2, 25 ± 2 and 45 ± 2 °C for 3 months. 2B and 3DS did not significantly change zeta potential at 4 ± 2 °C after storage for 1 month. At the end of the experiment, the zeta potential of 2DS at the beginning was significantly increased to −63.83 ± 1.79 and −58.93 ± 0.23 at 4 ± 2 and 25 ± 2 °C, respectively. Due to charged particle repulsion, drug delivery is more stable with higher zeta potentials, overcoming the natural impulse to aggregate. It is widely

Table 11
Active content of curcumin and alpha arbutin in nanoemulsions kept for 3 months.

Sample	Temperature (^{0}C)	%Remaining of curcumin				%Remaining of alpha arbutin			
		Initial	1 month	2 months	3 months	Initial	1 month	2 months	3 months
2B	4 ± 2		91.02	x	x		61.74	x	x
	25 ± 2	100	56.32	x	x	100	95.49	x	x
	45 ± 2		11.20	x	x		81.75	x	x
2DS	4 ± 2		98.35	95.73	94.69		96.30	95.73	90.45
	25 ± 2	100	84.96	82.32	81.38	100	99.08	93.76	90.08
	45 ± 2		90.25	x	x		92.22	x	x
3DS	4 ± 2		95.56	x	x		60.26	x	x
	25 ± 2	100	67.25	x	x	100	90.38	x	x
	45 ± 2		69.00	x	x		92.62	x	x
Curcumin in olive oil	4 ± 2		86.78	x	x	–	–	–	–
	25 ± 2	100	52.03	x	x	–	–	–	–
	45 ± 2		85.61	x	x	–	–	–	–
Curcumin in IPM	4 ± 2		81.65	80.06	79.23	–	–	–	–
	25 ± 2	100	84.23	78.74	77.89	–	–	–	–
	45 ± 2		79.79	x	x	–	–	–	–
Arbutin in distilled water	4 ± 2	–	–	–	–	100	90.53	89.90	87.76
	25 ± 2	–	–	–	–		96.86	90.23	86.27
	45 ± 2	–	–	–	–		98.09	x	x

Note: x = no investigate because of phase separation in nanoemulsion.

accepted that electrostatic stability requires zeta potentials greater than 30 mV [20]. The previous study also demonstrated that the high zeta potential of drug delivery systems may contributed to their great physical stability for long-term storage [20].

3.6. The active content of curcumin and alpha arbutin in stability test

The active content of curcumin and alpha arbutin in nanoemulsions kept for 3 months at various temperatures was shown in Table 11. After 1 month, all formulations had the highest content of curcumin at 4 ± 2 °C. 2B, 2DS and 3DS had the remaining content of 91.02, 98.35 and 95.56 % respectively. The samples of curcumin were also kept in isopropyl myristate (IPM) and olive oil, which were oil phases to prepare nanoemulsions, and the amount of their remaining content was compared in the stability test. After 3 months, 2DS found curcumin content of 94.69 and 81.38 % at temperatures of 4 ± 2 and 25 ± 2 °C, respectively, which was higher than curcumin kept in IPM (79.23 and 77.89 % at 4 ± 2 and 25 ± 2 °C, respectively). In the study of alpha-arbutin content after 1 month, it was found that 2B and 2DS had the highest content of arbutin at 25 ± 2 °C of 95.49 and 99.08 %, respectively, while 3DS had the highest content at 45 ± 2 °C of 92.62 %. The samples of alpha-arbutin were also kept in DI water to compare the remaining content in this study. After 3 months, it was found that 2DS had a similar content of alpha-arbutin at 90.45 and 90.08 % at 4 ± 2 and 25 ± 2 °C, respectively, which is higher than alpha-arbutin kept in DI water, which had a content of 87.76 and 86.27 % at 4 ± 2 and 25 ± 2 °C, respectively. During storage, unfavorable environments may occur, which degrade or alter the chemical components of the product, thereby decreasing their activity [51]. Hence, it is necessary for every formulation to ensure the stability of the active ingredients while maintaining their bioactivities. Under various unfavorable environments, the multiphase nanoemulsion successfully slowed the degradation of hydrophilic and hydrophobic compounds, which offered superior protection than single-phase emulsions or solutions [52]. In addition, it has been found that multiphase emulsions also protected co-loaded nutraceuticals against degradation by providing effective protective action [53]. Therefore, curcumin and arbutin were more stable when prepared into multiple nanoemulsions compared to active compounds kept in vehicles. In this study, the low temperature of 4 ± 2 °C was suitable for keeping high amounts of both active contents in multiple nanoemulsions.

4. Conclusion

This study examined a skin-whitening nanoemulsion that contained active compounds based on their synergistic tyrosinase inhibitory activity. The tyrosinase inhibition with substrate l-tyrosine from the mixture of curcumin and alpha-arbutin had the maximum activity with a synergistic effect at a CI value of 0.99. Preliminary emulsions prepared by the low-energy method were further developed into multiple nanoemulsions prepared using high energy to store synergistic active contents for tyrosinase inhibition. 2DS which was the most stable formulation, had a nanometer-scale interior droplet shape under TEM investigation. This formulation did not phase separate and had similar particle size, polydispersity index (PDI), zeta potential and pH values after 3 months of storage. In addition, curcumin and arbutin were preserved at 94.69 and 90.45 %, respectively at 4 °C for 3 months in multiple nanoemulsions. In $B_{16}F_{10}$, 2DS at 0.05 g/ml showed no cell cytotoxicity and anti-melanogenesis at 57.75 ± 5.74 %. The active compounds were formed into multiple nanoemulsions as a model delivery system to improve their efficacy and stability. The bio-synergistic activity of multiple nanoemulsions in this study might be further utilized in the development of novel health care and cosmetic products.

Data availability statement

Data will be made available on request.

CRediT authorship contribution statement

Mathukorn Sainakham: Writing – review & editing, Writing – original draft, Supervision, Project administration, Methodology, Funding acquisition, Formal analysis, Conceptualization. **Bouachompoo Promma:** Writing – original draft, Validation, Investigation, Data curation. **Arthima Ngernthong:** Writing – original draft, Validation, Investigation, Data curation. **Kanokwan Kiattisin:** Supervision, Formal analysis, Data curation. **Korawinwich Boonpisuttinant:** Methodology, Formal analysis, Data curation. **Krisada Wuttikul:** Methodology, Formal analysis, Data curation. **Pensak Jantrawut:** Validation, Conceptualization. **Warintorn Ruksiriwanich:** Validation, Conceptualization.

Declaration of competing interest

The authors declare that they have no known competing financial interests or personal relationships that could have appeared to influence the work reported in this paper.

Acknowledgements

This research project is supported by Faculty of Pharmacy, Chiang Mai University, and partially supported from Chiang Mai University.

References

[1] A. Di Petrillo, A.M. González-Paramás, B. Era, R. Medda, F. Pintus, C. Santos-Buelga, A. Fais, Tyrosinase inhibition and antioxidant properties of Asphodelus microcarpus extracts, BMC Compl. Alternative Med. 16 (2016) 1–9.
[2] L. Panzella, A. Napolitano, Natural and bioinspired phenolic compounds as tyrosinase inhibitors for the treatment of skin hyperpigmentation: recent advances, Cosmetics 6 (2019) 57.
[3] C. Niu, H.A. Aisa, Upregulation of melanogenesis and tyrosinase activity: potential agents for vitiligo, Molecules 22 (2017) 1303.
[4] J.P. Ebanks, R.R. Wickett, R.E. Boissy, Mechanisms regulating skin pigmentation: the rise and fall of complexion coloration, Int. J. Mol. Sci. 10 (2009) 4066–4087.
[5] T. Pillaiyar, M. Manickam, V. Namasivayam, Skin whitening agents: medicinal chemistry perspective of tyrosinase inhibitors, J. Enzym. Inhib. Med. Chem. 32 (2017) 403–425.
[6] G.L. Grove, A.M. Kligman, Age-associated changes in human epidermal cell renewal, J. Gerontol. 38 (1983) 137–142.
[7] Y. Matoba, T. Kumagai, A. Yamamoto, H. Yoshitsu, M. Sugiyama, Crystallographic evidence that the dinuclear copper center of tyrosinase is flexible during catalysis, J. Biol. Chem. 281 (2006) 8981–8990.
[8] R. Sarkar, S. Chugh, V.K. Garg, Newer and upcoming therapies for melasma, Indian J. Dermatol. Venereol. Leprol. 78 (2012) 417.
[9] J. García-Gavín, D. González-Vilas, V. Fernández-Redondo, J. Toribio, Pigmented contact dermatitis due to kojic acid. A paradoxical side effect of a skin lightener, Contact Dermatitis 62 (2010) 63–64.
[10] D. Chanchal, S. Swarnlata, Novel approaches in herbal cosmetics, J. Cosmet. Dermatol. 7 (2008) 89–95.
[11] E. Altuntaş, G. Yener, B. Özkan, Nanocarriers systems and their application for the delivery of different phytoconstituents, in: Novel Drug Delivery Systems for Phytoconstituents, 2019. Boca Raton.
[12] S. Gohtani, W. Prasert, Nano-emulsions; Emulsification using low energy methods, Japan J. Food Eng. 15 (2014) 119–130.
[13] C. Solans, P. Izquierdo, J. Nolla, N. Azemar, M.J. Garcia-Celma, Nano-emulsions, Curr. Opin. Colloid Interface Sci. 10 (2005) 102–110.
[14] N. Uson, M.J. Garcia, C. Solans, Formation of water-in-oil (W/O) nano-emulsions in a water/mixed non-ionic surfactant/oil systems prepared by a low-energy emulsification method, Colloids Sur. A Physicochem, Eng. Asp. 250 (2004) 415–421.
[15] T. Sheth, S. Seshadri, T. Prileszky, M.E. Helgeson, Multiple nanoemulsions, Nat. Rev. Mater. 5 (2020) 214–228.
[16] P. Linsaenkart, W. Ruksiriwanich, P. Jantrawut, C. Chittasupho, P. Rachtanapun, K. Jantanasakulwong, S.R. Sommano, C. Prom-U-Thai, S. Jamjod, C. Arjin, Natural melanogenesis inhibitor, antioxidant, and collagen biosynthesis stimulator of phytochemicals in rice bran and husk extracts from purple glutinous rice (Oryza sativa L. Cv. Pieisu 1 CMU) for cosmetic application, Plants 12 (2023) 970.
[17] Y. Wang, M.M. Hao, Y. Sun, L.F. Wang, H. Wang, Y.J. Zhang, H.Y. Li, P.W. Zhuang, Z. Yang, Synergistic promotion on tyrosinase inhibition by antioxidants, Molecules 23 (2018) 106.
[18] J.M. Morais, O.D. Santos, J.R. Nunes, C.F. Zanatta, P.A. Rocha-Filho, W/O/W multiple emulsions obtained by one-step emulsification method and evaluation of the involved variables, J. Dispersion Sci. Technol. 29 (2008) 63–69.
[19] R. Raviadaran, M.H. Ng, S. Manickam, D. Chandran, Ultrasound-assisted production of palm oil-based isotonic W/O/W multiple nanoemulsion encapsulating both hydrophobic tocotrienols and hydrophilic caffeic acid with enhanced stability using oil-based Sucragel, Ultrason. Sonochem. 64 (2020) 104995.
[20] M. Sainakham, A. Manosroi, M. Abe, W. Manosroi, J. Manosroi, Potent *in vivo* anticancer activity and stability of liposomes encapsulated with semi-purified Job's tear (*Coix lacryma*-jobi Linn.) extracts on human colon adenocarcinoma (HT-29) xenografted mice, Drug Deliv. 23 (2016) 3399–3407.
[21] K. Wuttikul, P. Boonme, Formation of microemulsions for using as cosmeceutical delivery systems: effects of various components and characteristics of some formulations, Drug Deliv. Transl. Res. 6 (2016) 254–262.
[22] P. O-chongpian, M. Na Takuathung, C. Chittasupho, W. Ruksiriwanich, T. Chaiwarit, P. Baipaywad, P. Jantrawut, Composite nanocellulose fibers-based hydrogels loading clindamycin HCl with Ca2+ and citric acid as crosslinking agents for pharmaceutical applications, Polymers 13 (2021) 4423.
[23] R. Chutoprapat, W. Malilas, R. Rakkaew, S. Udompong, K. Boonpisuttinant, Collagen biosynthesis stimulation and anti-melanogenesis of Bambara groundnut (Vigna subterranea) extracts, Pharm. Biol. 58 (2020) 1023–1031.
[24] P. Ma, Q. Zeng, K. Tai, X. He, Y. Yao, X. Hong, F. Yuan, Development of stable curcumin nanoemulsions: effects of emulsifier type and surfactant-to-oil ratios, J. Food Sci. Technol. 55 (2018) 3485–3497.
[25] P. Alam, S. Alqasoumi, F. Shakeel, M. Abdel-Kader, HPTLC densitometric analysis of arbutin in bulk drug and methanolic extracts of Arctostaphylos uva-ursi, Nat. Prod. Res. 25 (2011) 1671–1675.
[26] Y. Nazir, H. Rafique, N. Kausar, Q. Abbas, Z. Ashraf, P. Rachtanapun, K. Jantanasakulwong, W. Ruksiriwanich, Methoxy-substituted tyramine derivatives synthesis, computational studies and tyrosinase inhibitory kinetics, Molecules 26 (2021) 2477.

[27] F. Miao, M.Y. Su, S. Jiang, L.F. Luo, Y. Shi, T.C. Lei, Intramelanocytic acidification plays a role in the antimelanogenic and antioxidative properties of vitamin C and its derivatives, Oxid. Med. Cell. Longev. 2019 (2019).
[28] C.X. Tu, M. Lin, S.S. Lu, X.Y. Qi, R.X. Zhang, Y.Y. Zhang, Curcumin inhibits melanogenesis in human melanocytes, Phytother Res. 26 (2012) 174–179.
[29] D. Skroza, I.G. Mekinić, S. Svilović, V. Šimat, V. Katalinić, Investigation of the potential synergistic effect of resveratrol with other phenolic compounds: a case of binary phenolic mixtures, J. Food Compos. Anal. 38 (2015) 13–18.
[30] S. Zolghadri, A. Bahrami, M.T. Hassan Khan, J. Munoz Munoz, F. Garcia Molina, F. Garcia Canovas, A.A. Saboury, A comprehensive review on tyrosinase inhibitors, J. Enzym. Inhib. Med. Chem. 34 (2019) 279–309.
[31] X. Zhu, Y. Tian, W. Zhang, T. Zhang, C. Guang, W. Mu, Recent progress on biological production of α-arbutin, Appl. Microbiol. Biotechnol. 102 (2018) 8145–8152.
[32] S. Choi, Y.I. Park, S.K. Lee, J.E. Kim, M.H. Chung, Aloesin inhibits hyperpigmentation induced by UV radiation, Clin. Exp. Dermatol. 27 (2002) 513–515.
[33] D.J. Burgess, J.K. Yoon, Interfacial tension studies on surfactant systems at the aqueous/perfluorocarbon interface, Colloids Surf., B 1 (1993) 283–293.
[34] F.O. Opawale, D.J. Burgess, Influence of interfacial rheological properties of mixed emulsifier films on the stability of water-in-oil-in-water emulsions, J. Pharm. Pharmacol. 50 (1998) 965–973.
[35] M.M. Young, A. Franken, J.L. Du Plessis, Transepidermal water loss, stratum corneum hydration, and skin surface pH of female African and Caucasian nursing students, Skin Res, Technol. 25 (2019) 88–95.
[36] A. Rezk, A. Al-Hashimi, W. John, H. Schepker, M.S. Ullrich, K. Brix, Assessment of cytotoxicity exerted by leaf extracts from plants of the genus Rhododendron towards epidermal keratinocytes and intestine epithelial cells, BMC Compl. Alternative Med. 15 (2015) 1–18.
[37] V. Kahn, Effect of kojic acid on the oxidation of DL-DOPA, norepinephrine, and dopamine by mushroom tyrosinase, Pigm. Cell Res. 8 (1995) 234–240.
[38] L. Mungmai, C. Kanokwattananon, S. Thakang, A. Nakkrathok, P. Srisuksomwong, P. Tanamatayarat, Physicochemical properties, antioxidant and anti-tyrosinase activities of Durio zibethinus Murray and value added for cosmetic product formulation, Cosmetics 10 (2023) 87.
[39] P. Srisuksomwong, L. Kaenhin, L. Mungmai, Collagenase and tyrosinase inhibitory activities and stability of facial cream formulation containing cashew leaf extract, Cosmetics 10 (2023) 17.
[40] R. Mov, Comparative efficacy and safety of deoxyarbutin, a new tyrosinase-inhibiting agent, J. Cosmet. Sci. 57 (2006) 291–308.
[41] W. Wang, Y. Gao, W. Wang, J. Zhang, J. Yin, T. Le, J. Xue, U.H. Engelhardt, H. Jiang, Kojic acid showed consistent inhibitory activity on tyrosinase from mushroom and in cultured B16F10 cells compared with arbutins, Antioxidants 11 (2022) 502.
[42] J.H. Lee, J.Y. Jang, C. Park, B.W. Kim, Y.H. Choi, B.T. Choi, Curcumin suppresses α-melanocyte stimulating hormone-stimulated melanogenesis in B16F10 cells, Int. J. Mol. Med. 26 (2010) 101–106.
[43] K. Sugimoto, T. Nishimura, K. Nomura, K. Sugimoto, T. Kuriki, Inhibitory effects of α-arbutin on melanin synthesis in cultured human melanoma cells and a three-dimensional human skin model, Biol. Pharm. Bull. 27 (2004) 510–514.
[44] A. Eichner, S. Stahlberg, S. Sonnenberger, S. Lange, B. Dobner, A. Ostermann, T.E. Schrader, T. Hauß, A. Schroeter, D. Huster, Influence of the penetration enhancer isopropyl myristate on stratum corneum lipid model membranes revealed by neutron diffraction and 2H NMR experiments, Biochim. Biophys. Acta. Biomembr. 1859 (2017) 745–755.
[45] P. Ravikumar, P. Tatke, Advances in encapsulated dermal formulations in chemoprevention of melanoma: an overview, J. Cosmet. Dermatol. 18 (2019) 1606–1612.
[46] S. Soleymani, A. Iranpanah, F. Najafi, T. Belwal, S. Ramola, Z. Abbasabadi, S. Momtaz, M.H. Farzaei, Implications of grape extract and its nanoformulated bioactive agent resveratrol against skin disorders, Arch. Dermatol. Res. 311 (2019) 577–588.
[47] S. Roy, R. Priyadarshi, P. Ezati, J.W. Rhim, Curcumin and its uses in active and smart food packaging applications-A comprehensive review, Food Chem. 375 (2022) 131885.
[48] N. Aliabbasi, M. Fathi, Z. Emam-Djomeh, Curcumin: a promising bioactive agent for application in food packaging systems, J. Environ. Chem. Eng. 9 (2021) 105520.
[49] J. Komaiko, D.J. McClements, Optimization of isothermal low-energy nanoemulsion formation: hydrocarbon oil, non-ionic surfactant, and water systems, J. Colloid Interface Sci. 425 (2014) 59–66.
[50] M. Guttoff, A.H. Saberi, D.J. McClements, Formation of vitamin D nanoemulsion-based delivery systems by spontaneous emulsification: factors affecting particle size and stability, Food Chem. 171 (2015) 117–122.
[51] J.A. Rothwell, A. Medina-Remón, J. Pérez-Jiménez, V. Neveu, V. Knaze, N. Slimani, A. Scalbert, Effects of food processing on polyphenol contents: a systematic analysis using Phenol-Explorer data, Mol. Nutr. Food Res. 59 (2015) 160–170.
[52] H. Huang, T. Belwal, S. Liu, Z. Duan, Z. Luo, Novel multi-phase nano-emulsion preparation for co-loading hydrophilic arbutin and hydrophobic coumaric acid using hydrocolloids, Food Hydrocolloids 93 (2019) 92–101.
[53] L. Zou, W. Liu, C. Liu, H. Xiao, D.J. McClements, Designing excipient emulsions to increase nutraceutical bioavailability: emulsifier type influences curcumin stability and bioaccessibility by altering gastrointestinal fate, Food Funct. 6 (2015) 2475–2486.